SIMULATIONS OF SOLAR PORES

Cameron, R., Vögler, A.,* Schüssler, M., and Zakharov, V.

Max-Planck Institute for Solar System Research, 37191 Katlenburg-Lindau, Germany

ABSTRACT

We have used the MURaM code to simulate solar pores. These are magnetic features intermediate in size between the small-scale flux concentrations in the inter-granular lanes and sunspots. They appear only in young active regions and thus their formation seems not to be dominated by processes occurring in the photosphere. We therefore start the simulations with pre-existing pores and study their structure and evolution resulting from the effects of granular convection and radiative cooling. The simulations, unlike observations, allow the full 3-D structure to be examined, and various physical effects to be disentangled.

We find a reasonable agreement between the temperature and density stratification obtained in the simulations and those reported by observers. We shall present results concerning the magnetic and thermal structure of the simulated pores, their temporal evolution, and a number of synthetic diagnostics, such as intensity images at different wavelengths and limb distances.

Key words: Pores; Magnetic fields .

1. INTRODUCTION

Magnetic fields appear on the face of the Sun in such a variety of forms that the phrase "Solar dermatology" has come into (semi-)popular use. There is both an intrinsic interest in understanding each manifestation of the magnetic fields, and an interest due to the fact that the large scale properties of the chomosphere and corona and their coupling to the solar interior can only be understood by understanding individual processes. The use of "realistic" simulations which can be directly compared with observations was pioneered by Nordlund (1982, 1983) who successfully explained many of the properties of granulation and some aspects of magnetic field concentrations. The review by Steiner in these proceedings deals with the impressive successes which have recently improved our understanding of the smaller-scale features. In this paper we discuss simulations of pores, slightly larger features which have a well-formed stable umbra but which lack the complexities associated with a sunspot's penumbra. On the other hand they are considerably larger and longer lived than the micropores which appear in the simulations of Bercik et al. (2003) and Vögler et al. (2005)

Our simulations deal with the interaction between convective motions, magnetic fields, radiation and partial ionization in the layers near the photosphere. A brief overview of the physical problem and the numerical code is given in section 2. As such our simulations can and will be compared directly against observations, however it also means that we do not include processes which occur on the global scale of the Sun. The formation of pores falls into this class since, like sunspots, they do not spontaneously form in either our simulations or in the Quiet Sun but are associated with active regions and emerging flux regions (EFRs). For this reason we deal only with the surface properties of a well-developed pore and its decay. Section 3 will describe the way in which we have generated an initial condition. In section 4 we will then present our results - a snapshot of the solution and a comparison with the observations of Sütterlin (1998).

2. THE MURAM CODE.

The MURaM code Vögler et al. (2005) is designed to perform simulations of the solar photosphere and upper convection zone. It includes the necessary physics for a 'realistic' simulation of this layer of the solar atmosphere. The four basic equations the code treats are the momentum equation, the induction equation, the energy equation and an equation of state. These equations are all treated in the LTE approximation and the effects of multi-wavelength radiative transfer and partial ionization are included.

The code has been used to simulate granulation and small magnetic flux concentrations (Vögler et al. 2005; Vögler 2004); and synthesized line profiles generated by post-processing the simulation results (Schüssler et al. 2003;

*Present adress:HAO, National Center for Atmospheric Research, P.O. Box 3000, Boulder, CO 80307

Shelyag et al. 2004; Khomenko et al. 2004) provide a good match with the observations, as do center to limb studies (Keller et al. 2004).

3. IMPOSING A PORE: THE INITIAL CONDITION

As stated in the introduction, pores are not purely a surface phenomenon. They are associated with the solar cycle and the dynamo which is presumed to operate in the tachocline. For this reason we cannot expect a pore to spontaneously form in our limited simulation domain but must impose it a priori. We must then wait for the pore to reach a quasi-steady state (allowing for its natural decay). This is a non-trivial thing to do since the decay time for the pore turns out to be significantly shorter than the thermal relaxation time for the system. For this reason the pore must be nearly thermally relaxed when we begin the calculation. This then requires a carefully constructed initial condition; we will now sketch the procedure we have used to generate this initial condition.

The essential idea is to perform the initial calculation in 2-D where the magnetic concentration is both more stable and the simulation is less costly. We therefore begin with a non-magnetic simulation which has evolved to a statistically stationary state. The motions are then set to zero in the region where we insert the magnetic field, and a uniform field of 2kG is inserted. The boundary condition at the bottom of the magnetic region is changed so that in regions of inflow the gas has a reduced temperature, simulating the fact that the pore extends much deeper than our simulation box. The simulation is then allowed to evolve for several hours, during which time the pore remains mostly coherent. This coherence is due to the fact that a downflow forms at the edge of the pore, presumably driven by the strong radiative cooling at the side-wall of the pore (Deinzer et al. 1984). This downflow is supplied with mass by an inwards flow from the granules near the pore, resulting in a type of small-scale collar flow. In 2-D this is very efficient in confining the flux, although a small amount does escape into the surrounding plasma.

Once the 2-D simulation has reached a quasi-static state, we use it to generate an axisymmetric 3-D configuration. Field which has left the pore is removed, and careful attention is paid to ensure $\nabla \cdot B = 0$. A small amount of noise is added to the velocity and energy fields in order to break the symmetry. In the particular run to be discussed here a small amount of uniform negative flux was also added.

The boundary conditions used for the runs shown here are those used by Vögler et al. (2005) modified as described above and with a potential-field boundary condition at the top of the computational box. The box is periodic in both horizontal directions and covers 12 Mm$\times$12 Mm. The vertical extent is 1.4 Mm, with approximately 0.6 Mm lying above the $\tau = 1$ surface. The calculation was performed using $288 \times 288 \times 100$ grid points.

4. RESULTS

A snapshot of the pore, approximately halfway during its decay phase, is shown in Fig. 1. Before looking at the details of this snapshot we comment on Fig. 2 which compares the simulated pore with the inversions of observational data in Sütterlin (1998). From left to right, the orange curves show the average density, temperature and pressure as a function of optical depth for the simulated pore (for this purpose the pore was defined as the central region in Fig. 1 where the intensity was less than 80% of the quiet Sun value). In each panel the three solid black curves indicate the inversions and the dashed curve the simulated quiet Sun. The three observational curves correspond to three pores which had average diameters of $4.5''$, $3''$ and $2''$. The averaged profiles appear to match best for a diameter of 2" which is consistent with the apparent diameter in Fig. 1. This good match leads us to believe that the simulation provides an acceptable model of the pore at the photospheric level.

We now return to Fig. 1 to examine the fine structure of the solutions. Beginning with the intensity image, we see that the pore is almost uniformly dark with a 50-60 percent reduction in its brightness compared with the quiet Sun. There is a marginally bright rim outlining the pore. In the simulations the outline is very smooth, whereas observations show a much more corrugated structure, perhaps this is related to the somewhat coarse resolution used in the simulation.

Another phenomenon seen in the intensity images is the broadening of the inter-granular lanes connected to the pore, and the formation of a micropore above and slightly to the right of the pore in Fig. 1. Both of these aspects are seen more clearly when we look at the vertical component of the magnetic field.

In the 2-D case the flux is contained by inward horizontal motions, which are driven by the downwards mass flux at the outer edge of the pore. In the 3-D case there is still a downflow at the edge of the pore, as is seen in the vertical velocity image, but now the argument that it drives a horizontal inflow breaks down in the inter-granular lanes. The flux therefore can slowly escape the pore along the intergranular lanes.

Also seen in the image of the vertical magnetic field is the fact that the field inside the pore is very inhomogeneous. This inhomogeneity is noticeably absent from the intensity image. High-resolution magnetic field measurements are required in order to test this observationally.

Turning next to the image of the field inclination, we see that the magnetic field is essentially vertical over most of the pore, becoming significantly inclined only at the rim. The inclination of the velocity inside the pore is mostly vertical, even though the velocities there are small. Hence most of the motions inside the pore are, as expected, along the field-lines.

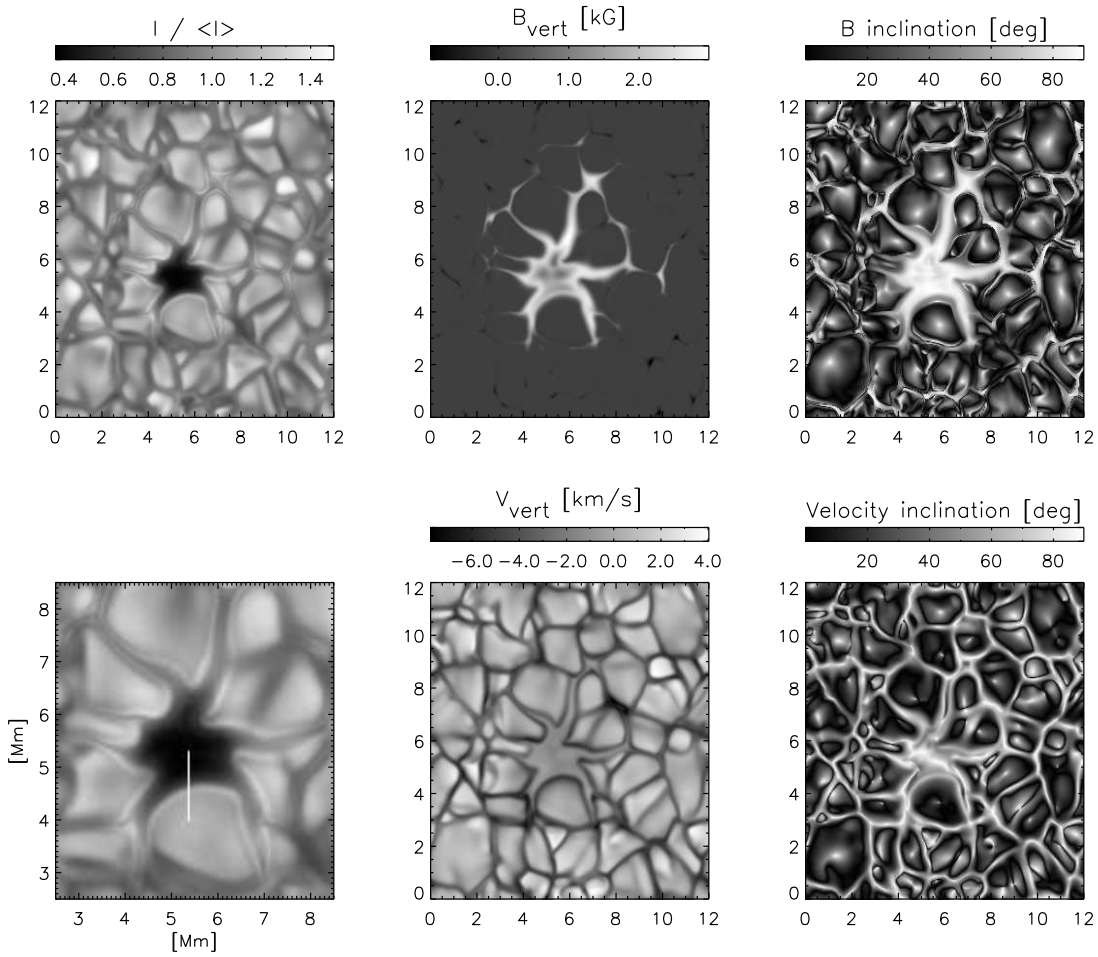

Figure 1. Shown (clockwise from the upper left) are the intensity, the vertical magnetic field, the inclination of the field from the solar surface, the inclination of the velocity, the vertical component of the velocity, and an enlargement of the region containing the pore. The intensity image has been normalized by the quiet Sun value. All quantities are shown on the $\tau = 1$ *surface.*

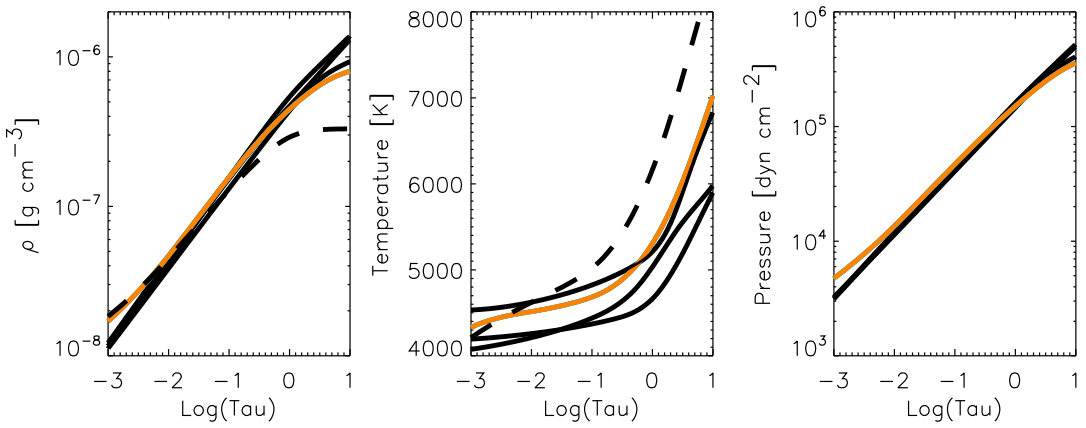

Figure 2. Shown in orange are the average density, temperature and pressure in the pore as a function of optical depth. For comparison the three solid black curves represent the results of inversions by Sütterlin of pore observations, and the dashed curve represents the quiet sun profiles. The match between the observations and the theory is good over a wide range of τ.

5. OUTLOOK

This paper has concentrated on some aspects of a pore simulation, focusing on a single snapshot in time. We have shown that the current simulations are in reasonably good agreement with observations. This work thus extends the range of magnetic features which be directly compared with simulations. In a future paper, currently in preparation, we intend to discuss both the time-development of the pore and the three dimensional structure of the solutions.

REFERENCES

Bercik, D. J., Nordlund, A., & Stein, R. F. 2003, in ESA SP-517: GONG+ 2002. Local and Global Helioseismology: the Present and Future, 201

Deinzer, W., Hensler, G., Schuessler, M., & Weisshaar, E. 1984, A&A, 139, 426

Keller, C. U., Schüssler, M., Vögler, A., & Zakharov, V. 2004, ApJ, 607, L59

Khomenko, E. V., Shelyag, S., Solanki, S. K., Vögler, A., & Schüssler, M. 2004, in IAU Symposium, 635

Nordlund, A. 1982, A&A, 107, 1

Nordlund, A. 1983, in IAU Symp. 102: Solar and Stellar Magnetic Fields: Origins and Coronal Effects, 79

Schüssler, M., Shelyag, S., Berdyugina, S., Vögler, A., & Solanki, S. K. 2003, ApJ, 597, L173

Shelyag, S., Schüssler, M., Solanki, S. K., Berdyugina, S. V., & Vögler, A. 2004, A&A, 427, 335

Sütterlin, P. 1998, A&A, 333, 305

Vögler, A. 2004, in 35th COSPAR Scientific Assembly, 4067

Vögler, A., Shelyag, S., Schüssler, M., et al. 2005, A&A, 429, 335